Acta Polytechnica **27**(0):136–140, 2020
doi:10.14311/APP.2020.27.0136

available online at http://ojs.cvut.cz/ojs/index.php/app

COMPARISON OF TWO TECHNIQUES FOR EVALUATING SPHERICAL INDENTATION DATA

Aleš Materna*, Petr Haušild, Jan Ondráček

Czech Technical University in Prague, Faculty of Nuclear Sciences and Physical Engineering, Department of Materials, Trojanova 13, Praha 2, Czech Republic

* corresponding author: ales.materna@fjfi.cvut.cz

Abstract. Flow curves of 15Kh2MFA, Sv 08Kh19N10G2B and 08Kh18N10T steels used for fabrication of WWER-440 nuclear reactor pressure vessel and core internals were obtained using the automated ball indentation (ABI) test technique and compared with flow curves evaluated from the same measured load-displacement data and widely used Oliver-Pharr method. Differences in results obtained by both studied methods do not exceed 12 % and are attributed to the amount of material pile-up.

Keywords: Automatic ball indentation, Oliver-Pharr method, pile-up, true stress-strain curve.

1. Introduction

Perhaps the most important test of a material's mechanical response is the tensile test. For small volume of material, from which the standard tensile test specimens cannot be manufactured, one can use an instrumented indentation. For estimation of a stress-strain curve from indentation data, a spherical indenter has advantage among others with e.g. conical or pyramidal shapes. Contact angle of spherical indenter changes with loading (contrary to conical or pyramidal indenters), which allows determination of more than one point of the stress-strain curve. On the other hand, the shape of the ball limits the achieved strains to 0.2. At this limit value, both indent and ball diameters equal. There are numerous models available to reduce the spherical indentation data to uniaxial stress-strain behavior of the test material (e.g. [1–3]). They differ in the level of physical simplification and in the computational complexity. The accuracy of such models relies substantially on proper determination of the contact area between the indenter and test material.

The simple model based on the well-known Hertz law is suitable for low indentation forces, when the deformations under the indenter are elastic. A more advanced method was introduced by Oliver and Pharr (OP) [4], which calculates the projected contact area from elastic contact stiffness at peak load. This method, however, can lead to underestimation of the true contact area for materials exhibiting pile-up [5, 6]. To account for the material pile-up, the partial unloading technique and set of iterative equations was introduced by Haggag [7] in Automatic Ball Indentation (ABI) testing. After determination of the contact radius, two Tabor's expressions [8] can be used to obtain representative stress and strain. These indentation values should be equivalent to true stress-strain uniaxial ones.

In this work, the OP and the ABI techniques are compared on data sets obtained during the standard ABI test procedure with progressive indentation and intermediate partial unloadings. All materials involved in this study are used for manufacturing of pressure vessel and core internals of nuclear reactor of WWER-440 type.

2. Tested materials

Three various steels present at WWER 440 nuclear power plant reactor were involved in this study: (i) chromium-molybdenum-vanadium low alloy 15Kh2MFA steel, which is used as pressure vessel base metal, (ii) 19 chromium/10 nickel niobium-stabilized austenitic stainless steel Sv 08Kh19N10G2B, which is used as pressure vessel outer layer cladding, and, (iii) chromium-nickel titanium-stabilized austenitic stainless steel 08Kh18N10T, which is used as main structural material for the reactor internals (namely the core barrel, the core basket and the block of guide tubes). 08Kh18N10T steel was studied in two deformation states: (a) as manufactured, and, (b) cold-deformed with the thickness reduction 20 %.

3. Methods and analysis

Mechanical properties of all test materials were evaluated from load P - displacement h curve recorded during a progressive ball indentation with multiple intermediate partial-unloadings at one location on specimen's surface.

As a basis for evaluation, Tabor's relations between the representative strain ε_r and the representative stress σ_r on left sides and the contact diameter d and the applied force P during spherical indentation on the right side were used:

$$\varepsilon_r = 0.2\frac{d}{D}, \tag{1}$$

$$\sigma_r = \frac{4P}{\delta\pi d^2}, \tag{2}$$

where D is the indenter diameter, and δ is the constraint factor.

It follows from Equation (1) that strain up to a maximum value of 0.2 can be achieved. In that limit case the ball penetrates material surface to its full diameter ($d = D$). Representative values ε_r and σ_r are regarded as material true plastic strain ε_p and true stress σ_t.

During the instrumented indentation, contact diameter d is not directly measured and must be approximated from P - h curve. There are numerous approaches to that and two of them were chosen in this work for comparison.

3.1. Oliver-Pharr method

The most widely used method for determining elastic modulus from instrumented indentation data is Oliver-Pharr (OP) method [4], which evaluates contact diameter d as intermediate result from the contact depth h_c according to equations

$$d = 2\sqrt{h_c\,(D - h_c)}, \tag{3}$$

$$h_c = h_{max} - \varepsilon\frac{P_{max}}{S}. \tag{4}$$

Here, P_{max} is the force at maximum indentation depth h_{max}, $S{=}dP/dh|_{h\,=\,h_{max}}$ the initial unloading slope, and, constant $\varepsilon = 0.75$ for spherical indenter. The constraint factor δ in Equation (2) was set to 3 in this study.

3.2. Haggag method

Haggag in his ABI test procedure [7] uses Tabor's Equations (1) and (2), iteratively computed plastic indentation diameter d_p (after unloading) instead of d, and, the constraint factor δ in in Equation (2) dependent on the stage of deformation beneath the indenter. The value of d_p comes from the Hertz's classical theory and has the form

$$d_p = \sqrt[3]{0.5CD\frac{h_p^2 + \left(\frac{d_p}{2}\right)^2}{h_p^2 + \left(\frac{d_p}{2}\right)^2 - h_pD}}, \tag{5}$$

where the indentation depth after unloading h_p is extrapolated from measured unloading data and

$$C = 5.47 \cdot P\left(\frac{1}{E_1} + \frac{1}{E_2}\right), \tag{6}$$

where E_1 and E_2 are the Young's moduli for the indenter and test material, respectively. According to statistical analysis of many experimental data it was proposed by Francis [8] that the constraint factor δ in Equation 2 is a function of the indentation variable

$$\phi = \frac{\varepsilon_p E_2}{0.43\sigma_t}. \tag{7}$$

Contrary to Francis's work, the ABI procedure uses slightly modified functions for the constraint in the form:

$$\delta = \begin{cases} 1.12 & \Phi \le 1 \\ 1.12 + \tau\ln(\phi) & 1 < \Phi \le 27 \\ \delta_{\max} & \Phi > 27 \end{cases} \tag{8}$$

where $\delta_{max} = 2.87\alpha_{\mathrm{m}}$, $\tau = (\delta_{max}$ - 1.12)/ln(27) and α_{m} is the constraint factor index whose value varies between 0.9 and 1.25 for various structural steels. Since no experimental data were available for calibration, value $\alpha_{\mathrm{m}} = 1.1$ in the middle of the interval was used.

4. Experimental details

4.1. Mechanical testing

All ABI tests were carried out at room temperature using Inspekt 20 kN testing machine and custom-made testing device equipped with the replaceable tungsten-carbide ball and with two-arm extensometer for the measuring of the ball displacements. Two different ball diameters were used: 2.5 mm for testing of 15Kh2MFA and Sv 08Kh19N10G2B steels, 1.5 mm for 08Kh18N10T steel. Indentation loading sequence for each test material is evident from Figures 1-3.

For comparison purposes, standard tensile tests at room temperature using Inspekt 100 kN testing machine were performed for 15Kh2MFA and Sv 08Kh19N10G2B steels. Tensile test specimens of 6 mm diameter were oriented in circumferential direction of the pressure vessel that corresponds to the direction of the indentation.

4.2. Confocal microscopy

In order to determine the amount of pile-up, it was necessary to obtain the topography of the spherical indentation. The depth profile was measured with Olympus OLS5000-SAF confocal microscope employing a 405 nm wavelength laser diode.

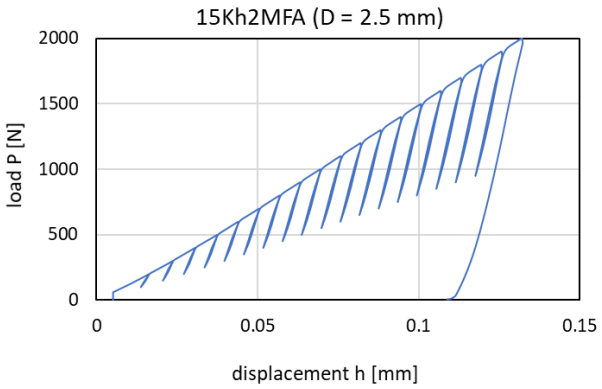

Figure 1. ABI test load - displacement curve for 15Kh2MFA steel.

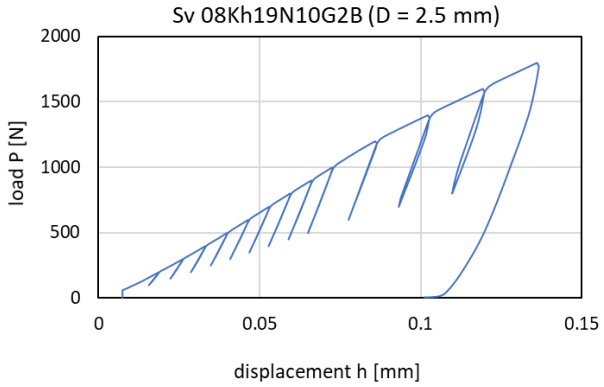

Figure 2. ABI test load - displacement curve for Sv 08Kh19N10G2B steel.

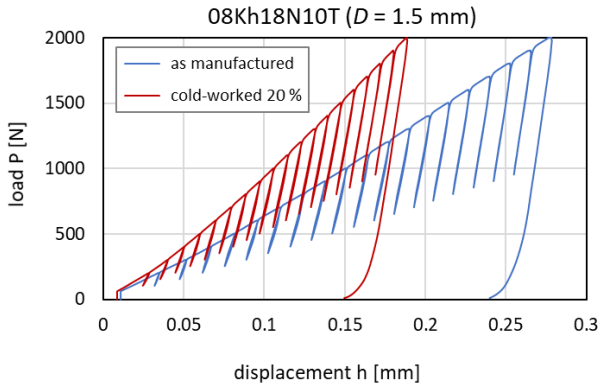

Figure 3. ABI test load - displacement curve for undeformed a cold deformed 08Kh18N10T steel.

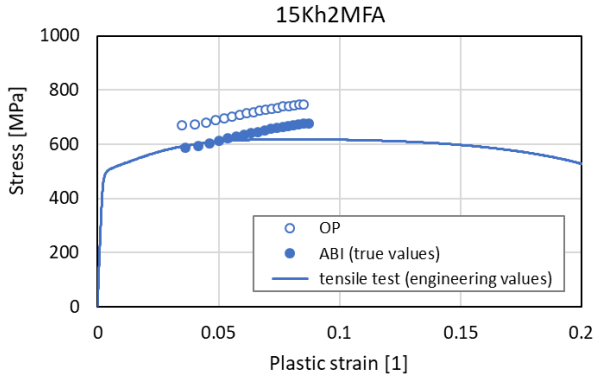

Figure 4. Stress/plastic strain curves for 15Kh2MFA steel obtained by various techniques.

5. Results and discussion

Measured load displacement curves are for 15Kh2MFA steel plotted in Figure 1, for Sv 08Kh19N10G2B steel in Figure 2 and for two deformation states of 08Kh18N10T steel in Figure 3. Evaluated points which form the true stress/plastic strain curves are for 15Kh2MFA steel plotted in Figure 4, for Sv 08Kh19N10G2B steel in Figure 5 and for two deformation states of 08Kh18N10T steel in Figure 6.

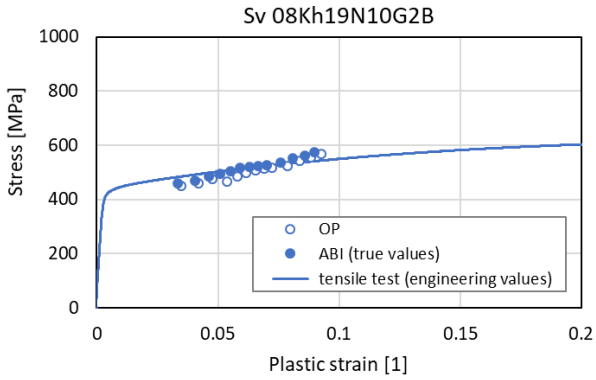

Figure 5. True stress/plastic strain curves for Sv 08Kh19N10G2B steel obtained by various techniques.

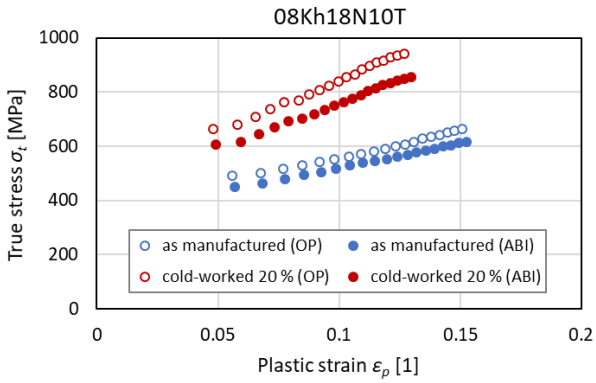

Figure 6. True stress/plastic strain curves for undeformed a cold deformed 08Kh18N10T steel.

Steels with higher hardness exhibit lower penetration depths at the same load level and the higher flow stresses at the same strain levels. It can be observed in Figure 3 and Figure 6 for 08Kh18N10T steel hardened by the cold working.

However, more important differences are between the curves in Figures 4 - 6 evaluated using simple Oliver-Pharr method and more sophisticated iterative ABI test method. Except the cladding material, OP leads to higher stresses and lower strains compared to the ABI technique. As can be seen in Figures 4 and 5, true stress-strain data points evaluated by ABI iterative procedure are in good agreement with standard tensile curves and this agreement can even be improved by the correction of tensile data to specimens necking.

One possible explanation for differences between the OP and ABI results lies in chosen standard values of constraint factors, which can be inaccurate for tested steels. Alternatively, it could be attributed to the amount of material pile-up or sink-in around the indent. In case of material pile-up, OP method underestimates the contact area which could lead to increase of estimated stresses.

It was proved experimentally in Figures 7 - 9,

where cross-sectional profiles for all indents are plotted. Whereas materials pile-up around the indents in 15Kh2MFA (Figure 7) and 08Kh18N10T (Figure 9) steels, surface around the indent in Sv 08Kh19N10G2B remains flat (Figure 8).

Susceptibility to pile-up can also be observed in P - h plots. For linear indenters (e.g. conical or pyramidal), high final-to-maximum depth ratio h_f/h_{max} > 0.8 indicates material pile-up [5]. For non-linear spherical indenter, the h_f/h_{max} criterion is not as straightforward, because the deformation state under the indenter depends on the depth of penetration. It starts in pure elastic regime with sink-in at small depths and ends in fully plastic regime with possible pile-up. From this point of view, 15Kh2MFA and Sv 08Kh19N10G2B steels are tested at the similar h/D ratios with expected higher h_f/h_{max} ratio for piling-up 15Kh2MFA steel (compare Figures 1 and 2). On the other hand, pile-up is typical for materials with higher elastic modulus-to-yield stress ratio E/σ_y, which is higher for Sv 08Kh19N10G2B comparing to 15Kh2MFA. This discrepancy in observed effect of the yield stress on pile-up occurrence can be attributed to ability of Sv 08Kh19N10G2B cladding to work-harden to much higher plastic strains comparing to 15Kh2MFA steel (compare tensile curves in Figures 4 and 5).

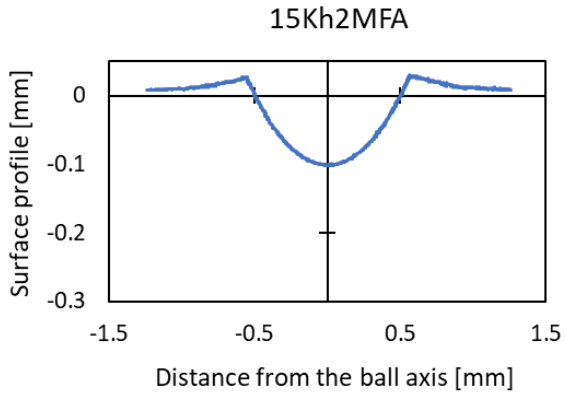

FIGURE 7. Cross-sectional profile of the spherical indent in 15Kh2MFA steel.

6. CONCLUSIONS

The instrumented spherical indentation was used for characterization of tensile properties of base metal (15Kh2MFA steel) and cladding (Sv 08Kh19N10G2B steel) of WWER-440 reactor pressure vessel and of main structural material of reactor core internals in two deformation states (undeformed and cold-deformed 08Kh18N10T steel). The aim of the study was to evaluate true stress/strain curves of all studied materials and to compare two methods of their evaluation: more complex ABI test iterative procedure proposed by Haggag and the relatively simple and available method of Oliver-Pharr mainly used

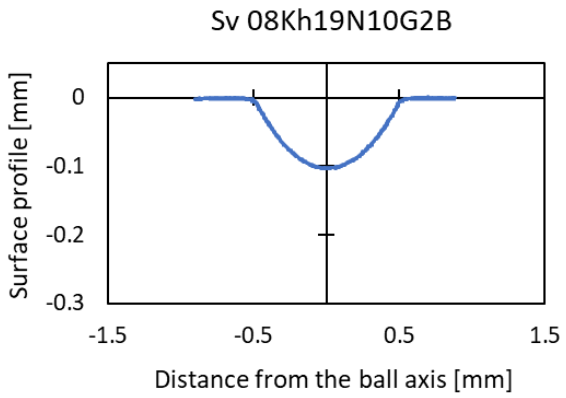

FIGURE 8. Cross-sectional profile of the spherical indent in Sv 08Kh19N10G2B steel.

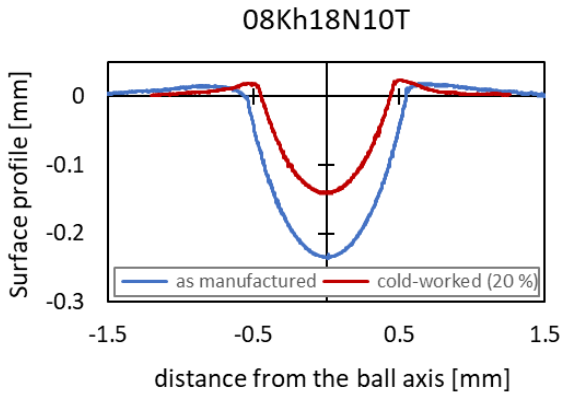

FIGURE 9. Cross-sectional profile of the spherical indent in undeformed a cold deformed 08Kh18N10T steel.

for determination of elastic modulus and hardness of materials.

Whereas tensile curves computed according to ABI equations match standard uniaxial tensile curves for 15Kh2MFA and Sv 08Kh19N10G2B steels, the OP method predicts about 12 % higher stresses for 15Kh2MFA steel and about 7 % and 11 % higher stresses for undeformed and cold-deformed 08Kh18N10T steel, respectively. These higher stresses are probably connected to the material pile-up, which has increased the real contact area contrary to the hypothetical one evaluated using simplified elastic assumptions of the OP model. In case of Sv 08Kh19N10G2B steel, no pile-up was observed and both methods led to similar results.

ACKNOWLEDGEMENTS

This work was supported by the Technology Agency of the Czech Republic under the project No. TH02020565 and by the European Structural and Investment Funds under the project CZ.02.1.01/0.0/0.0/16_019/0000778 (Centre of Advanced Applied Sciences).

References

[1] H. Francis. Phenomenological analysis of plastic spherical indentation. *Journal of Engineering Materials and Technology, Transactions of the ASME* **98**:272–281, 1976. doi:10.1115/1.3443378.

[2] P. Au, G. Lucas, J. Sheckherd, G. Odette. Flow property measurements from instrumented hardness tests. *Non-destructive evaluation in the nuclear industry* pp. 597–610, 1980.

[3] B. Taljat, T. Zacharia, F. Kosel. New analytical procedure to determine stress-strain curve from spherical indentation data. *International Journal of Solids and Structures* **35**(33):4411 – 4426, 1998. doi:10.1016/S0020-7683(97)00249-7.

[4] W. Oliver, G. Pharr. An improved technique for determining hardness and elastic modulus using load and displacement sensing indentation experiments. *Journal of Materials Research* **7**(6):1564–1583, 1992. doi:10.1557/JMR.1992.1564.

[5] A. Bolshakov, G. M. Pharr. Influences of pileup on the measurement of mechanical properties by load and depth sensing indentation techniques. *Journal of Materials Research* **13**(4):1049–1058, 1998. doi:10.1557/JMR.1998.0146.

[6] B. Taljat, G. Pharr. Development of pile-up during spherical indentation of elastic-plastic solids. *International Journal of Solids and Structures* **41**(14):3891 – 3904, 2004. doi:10.1016/j.ijsolstr.2004.02.033.

[7] F. Haggag. In situ measurement of mechanical properties using novel automated ball indentation system. *ASTM Special Technical Publication* pp. 27–44, 1993. doi:10.1520/STP12719S.

[8] D. Tabor. *The Hardness of Metals*. Clarendon Press, UK, 1951.